Jpn. J. Pharmacol. 72, 355–364 (1996)

New Algorithms for Real-Time, 24 hr Continuous and Noise-Adjusted Power Spectral Analysis of Heart Rate and Blood Pressure Fluctuations in Conscious Rats

Ryuji Nagai and Shinya Nagata

Department of Pharmacology I, Discovery Research Laboratories I, Dainippon Pharmaceutical Co., Ltd., Enoki 33–94, Suita, Osaka 564, Japan

Received July 12, 1996 Accepted September 27, 1996

ABSTRACT—The effective combination of C++ and assembler could realize real-time power spectral analysis of various fluctuation indexes simultaneously. The blood pressure (BP) waveform indexes (WIs) analyzed simultaneously were heart rate (HR), systolic blood pressure (SBP), mean blood pressure (MBP) and diastolic blood pressure (DBP). Power amplitudes (very low frequency, VLFamp; low frequency, LFamp; and high frequency, HFamp) were evaluated by accurate BP waveform recognition, accurate automatic rejection of outliers, baseline adjustment in periodograms and digital filtering of each amplitude. In the in vivo experiments, the amplitudes were changed in a dose-dependent manner by methylatropine (HR-VLFamp, HR-LFamp and HR-HFamp), phentolamine (HR-LFamp, SBP-VLFamp, SBP-LFamp and SBP-HFamp) and propranolol (HR-LFamp and SBP-LFamp). The absolute correlation coefficients of the amplitude and the change in each parameter were more than 0.96. In conclusion, this real-time, noise-adjusted power spectral analysis system for investigating HR and BP fluctuations enabled us to accurately evaluate autonomic nerve activity in conscious rats. Moreover, unlike other systems, this system was able to detect the biphasic changes in SBP-HFamps caused by phentolamine.

Keywords: Digital filter, Periodogram, Sympathetic nerve function, Parasympathetic nerve function, Autonomic nerve

Great effort has been focused on the estimation of autonomic function by power spectral analysis of HR and BP fluctuations (1–11). From pharmacological and physiological experiments, it is generally thought that HR-HFamp reflects primarily parasympathetic function (9, 10) and SBP-LFamp reflects sympathetic function (11). However, the lack of theoretical quantitative methods for power spectral calculation has caused many conflicting results. For example, the following disparate results were reported: significant decrease (1) vs little change (12) in HR-LFamp by atropine; slight increase (2, 13) vs slight decrease (12) in HR-HFamp by propranolol; increase in HR-LFamp (1) vs no increase in HR-LFamp (12) by an angiotensin-converting enzyme inhibitor. The FFT method (1) and power spectral estimation (maximum entropy method or autoregressive model) (13, 14) have been used for more accurate calculation of power spectra. However, can we achieve sufficiently accurate power spectra by only improving the mathematical calculation methods of frequency analysis?

Most current methods only use intermittent analysis even though the systems analyze small fractions of the entire data base and moreover sporadically detect fluctuations that can take place over a few minutes or a few seconds (1, 2, 15, 16). Ideally, a system that can realize real-time noise rejection, waveform recognition and power spectral analysis is preferred. Moreover, the ability to perform these functions with a personal computer makes experiments economically feasible. Kuo and Chan (17) has described a system that is able to realize continuous, on-line, real-time spectral analysis of BP signals; However, their method is based on the direct FFT of raw

Abbreviations used are: AOC, area over the curve; AUC, area under the curve; BP, blood pressure; DBP, diastolic blood pressure; FC, cut-off frequency; FFT, fast Fourier transform; HF(amp), high frequency (amplitude); HR, heart rate; LF(amp), low frequency (amplitude); MBP, mean blood pressure; SBP, systolic blood pressure; VLF(amp), very low frequency (amplitude); WI, waveform index.

BP signals without the time-consuming waveform recognition. Although the direct FFT method successfully solved some of the problems found with the off-line intermittent analytical system, it is not able to reject noise mathematically or differentiate HR, SBP, MBP and DBP fluctuations.

In the previous study, we developed a new algorithmic-based digital filter processing system that has a noise rejection function by Smirnov's rejection test and realized real-time continuous BP measurement and analysis in freely-moving conscious rats (18). In this study, we attempted to solve the problems in power spectral analysis by developing the system (18) with an effective combination of a machine language and an object-oriented programming language built into a personal computer. Furthermore, the accuracy of the system was evaluated with in vivo models by testing adrenergic and cholinergic receptor antagonists that affect autonomic function.

MATERIALS AND METHODS

Methods

For realizing noise-adjusted power spectral analysis, a previously reported algorithm (18) was applied. Briefly, the algorithm calculates a series of WIs, recognizes BP waveform and rejects noisy waveforms, performing all these functions simultaneously. Prior to FFT, the time series WIs were interpolated with an interval of 50 msec by using the 3 dimensional spline function. The spline function is effective in describing a smooth curve that can pass through all points, even though the intervals of these points are unequal. The simple average for each set of data, which consisted of 1024 interpolated values, was calculated and then subtracted from each interpolated value in that set of data. Because the data at both sides of the finite data set are discontinuous and the distorted spectrum is calculated (Gibbs' phenomenon), the Hamming window was used to attenuate Gibbs' phenomenon. Half of each data set was overlapped by the next set of data to attenuate the side effect of amplitude decrease on both sides of a set caused by the Hamming window (Fig. 1). The frequency bands of VLF, LF and HF were as described in the previous study (12). The VLFamp and LFamp of each periodogram were calculated as the area under the periodogram within the frequency range of 0.02–0.24 Hz and 0.26–0.74 Hz, respectively. The HFamp was determined as the area at 0.26 Hz before and after the center, which was the maximum value in the frequency range from 0.76 to 3.00 Hz in a periodogram (Fig. 2). The DC components (baseline amplitude) of the LF and HF were removed in each periodogram (Fig. 2).

Secondary infinite impulse response Butterworth digital filters were used for smoothing of all the amplitudes. An appropriate digital filter was created for each indicated time point, and the FC of that filter was then automatically determined from the intervals before and after the indicated time points. Figure 3 shows an example in the case of SBP-LFamp. Other amplitudes (i.e., SBP-VLF and SBP-HF) were calculated in the same way.

Algorithm

1) The FC is automatically determined from the interval between the indicated time points. The indicated time points are determined according to the study needs of the operator after collecting data. For instance, if the indicated time points are 10, 30 and 60 min after the reference time point (e.g., drug administration time), the FC for the 10, 30 and 60 min time points are calculated as 1 / (10 min − 0 min) = 0.00166 Hz, 1 / (30 min − 10 min) = 0.000833 Hz and 1 / (60 min − 30 min) = 0.000555 Hz, respectively.

2) The amplitudes during the previous and the following indicated time points are filtered by the digital filter for the indicated time point. In Fig. 3, the amplitudes during 0 and 30 min are filtered by the filter for 10 min. The amplitudes during 10 and 60 min are filtered by the filter for 30 min. The amplitudes during 30 and 120 min are filtered by the filter for 60 min.

3) Delay-time compensations to the digital filter out-

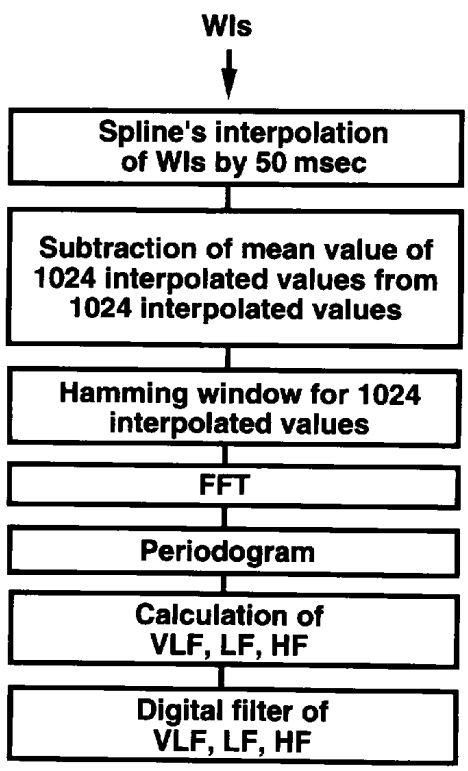

Fig. 1. Overview for procedure of the algorithm.

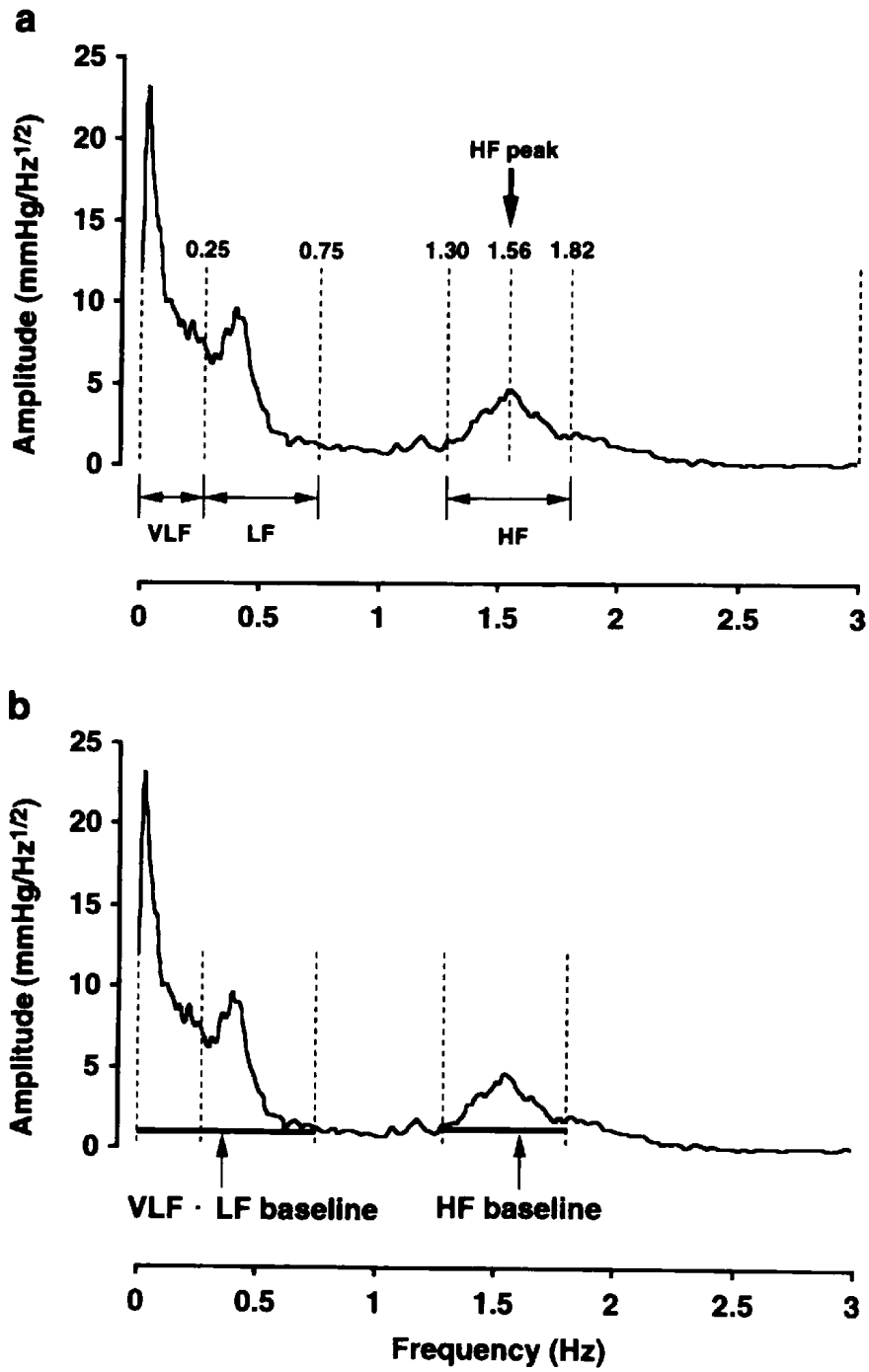

Fig. 2. Calculation of each periodogram. a: Segmentation for VLFamp, LFamp and HFamp in a periodogram (solid line). The VLFamp and LFamp were integrated within 0.02–0.24 Hz and 0.26–0.74 Hz, respectively. The HFamp area was determined as the area 0.26 Hz before and after the maximum value in the frequency range from 0.76 to 3.00 Hz in a periodogram, and the HFamp was integrated in that HFamp area. b: Determination of VLF·LF and HF baselines.

puts are applied. The compensation error can be ignored because it is negligible in terms of the FC cycle. For example, when the amplitudes are sampled for every 25.6 sec, i.e., the FS (sampling frequency) is 0.039 Hz and the FC for 10 min time point is 0.00166 Hz, the delay-time is about 146.43 sec (the maximum is 169.17 sec and the minimum is 125.30 sec), and the digital filter outputs are uniformly shifted ahead about 146.43 sec. The maximum compensation error of about 23 sec, which is the difference between 146.43 and 169.17 sec or 146.43 and 125.30

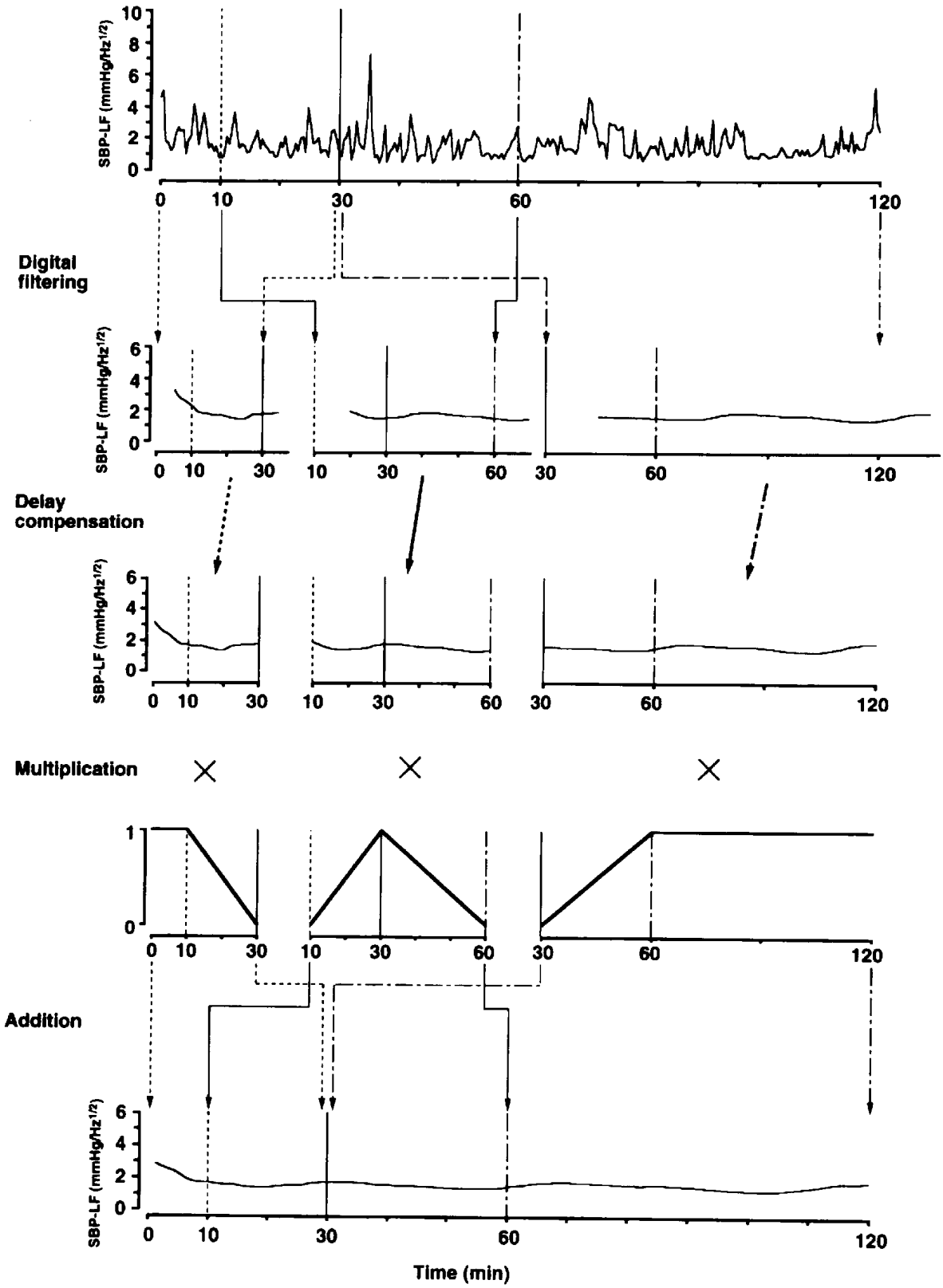

Fig. 3. For 120 min SBP-LFamp values, the representative SBP-LFamps of 10, 30 and 60 min time points were determined as follows: 0–30, 10–60 and 30–120 min areas were set for each of the indicated time points and filtered by adequate digital filters for the indicated time points. Each of the filtered data was compensated and multiplied by the weighted function and added. The representative SBP-LFamps were determined from the result data at 10, 30 and 60 min.

sec, is considered to be insignificant (about 1.7%) considering that the FC cycle is 600 sec. Similarly, the compensation time for 30 and 60 min time points are 434.64 and 868.41 sec, respectively.

4) The weighting function is performed by constructing two consecutive linear functions whose specifications are 1 at each indicated time point and 0 at the previous and the following time points. However, if there is no previous or following time point, the first or last linear function has a constant of 1. The weighting functions are then multiplied by the compensated digital filter outputs, and the results are added (Fig. 3). The representative amplitudes are determined from the data at the indicated time points.

Hardware

The system hardware was as follows: computer (PC-H98 Model 90; NEC, Tokyo) with CPU (i80486SX 25 MHz; Intel, Santa Clara, CA, USA); an over-drive processor (DX4, Intel); 100 MB hard disk and 13.6 MB memory; 5-inch MO disk drive (PC-OD0101, NEC); A/D converter board (ADM-1698BPC; Micro Science Co., Ltd., Tokyo); load-cell converters as BP measuring amplifiers (LC210 A/Z; Unipulse Co., Ltd., Saitama); disposable BP transducers (DX-360; Nihon Kohden Co., Ltd., Tokyo); watertight swivels (BC-101; Biomedica, Osaka); automated heparin injection machine (DAI-1; Labo Support, Osaka). The resonance frequency of this BP measuring is 35.7Hz, and the damping coefficient is 1.98.

Animals

Std:Wistar rats (Japan SLC, Inc., Shizuoka; 15-weeks-old, 300−350 g) were implanted under anesthesia with abdominal aortic and venous (jugular vein) polyethylene catheters (SP-31; Natsume, Tokyo) filled with saline containing heparin. The catheters were passed subcutaneously and pulled out from the dorsal neck and attached to watertight swivels. Drugs were administered via the jugular vein the day after catheter implantation. The rats were housed individually in suspended wire-mesh cages. The room was lit from 7:00 AM to 7:00 PM. Temperature (23±2℃) and humidity (55±5%) were kept constant. Food (pellet form) and bottles with stainless-steel drinking spouts were available ad libitum.

Drugs

Concentrations and administration routes were as follows: methylatropine (Sigma Chemical Co., St. Louis, MO, USA; 0.1, 0.3, 1, 3 mg/kg), phentolamine (Ciba-Geigy Japan, Hyogo; 0.1, 0.3, 1, 3, 10 mg/kg) and propranolol (Sigma Chemical Co.; 1, 3, 10 mg/kg) were administered by bolus intravenous injection into the venous catheter. A rat was administered only one drug at a concentration. Drugs were administered after each frequency component attained a steady level (about 3 hr after administration). A 0.2-ml vol of heparin (Dainippon Pharmaceutical Co., Ltd., Osaka; 100 U/ml) was injected for 0.1 sec every 3 hr into the aortic catheter with an automated injection machine.

Statistical analyses

R values were determined by the correlation coefficient of the least-squares linear-regression analysis. Each point in Fig. 7 represents the mean ±S.E. of 6−8 different rats. The size of the symbol increases as the dose increases. All S.E. values are smaller than 0.28, and all S.E. bars are behind the symbols.

RESULTS

Simulation and raw data

Four sets of the real HR data for 500 sec were combined and the artificial HR data for 2,000 sec were made. The simulation model demonstrated that a rectangular pulse (duration 2 sec) added to the artificial HR data changed a normal power spectrum to an abnormal one (Fig. 4). The abnormal LFamp was higher than the normal one, because the baseline amplitude was elevated in the LF area in an abnormal power spectra. When LFamp was calculated from the weighted averaging method with digital filters, each amplitude was remained steady (Fig. 4). Figure 5 shows the continuous changes of SBP and SBP-LFamps calculated from the periodogram, power spectrum and the weighted averaging method with digital filters when phentolamine (3 mg/kg, i.v.) was administered in a conscious rat. The two power spectral analysis methods were compared in the real SBP data for 22 hr collected from an actual in vivo model (Fig. 5: c and d). Figure 6 shows the comparison between the weighted averaging method with digital filters and the existing calculation method. Data were collected for 27 hr under the conscious condition. Especially, not able are the results that the HFamps calculated from the weighted averaging method with digital filters are larger than those from the existing calculation method (Fig. 6).

Quantitative test

The correlation coefficients (r values) were calculated to evaluate the quantitative accuracy of this method. The changes in AOC or AUC of each parameter were used as the incidence (Fig. 7). Phentolamine reduced BP, increased HR and changed all amplitudes in a dose-dependent manner. MBP change was used as an incidence for the calculation of r values. Phentolamine decreased HR-LFamp ($r=0.98$) and changed HR-HFamp in a biphasic

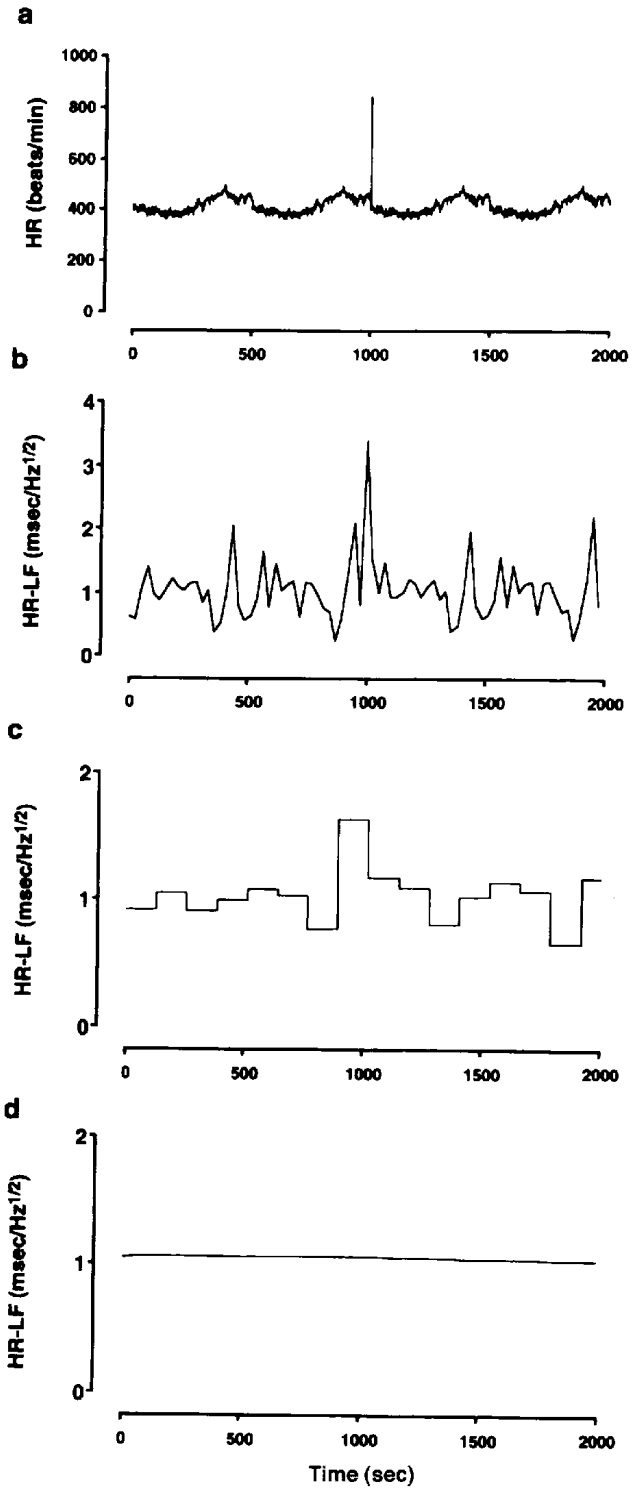

Fig. 4. Comparison between the usual power spectral calculation method and the weighted averaging method with digital filters. a: Four sets of the real HR data for 500 sec were combined, and the artificial HR data for 2,000 sec were made. Time course of HR-LFamp in the periodogram (b), HR-LFamp calculated from the usual power spectral calculation method (c) and HR-LFamp calculated from the weighted averaging method with digital filters (d).

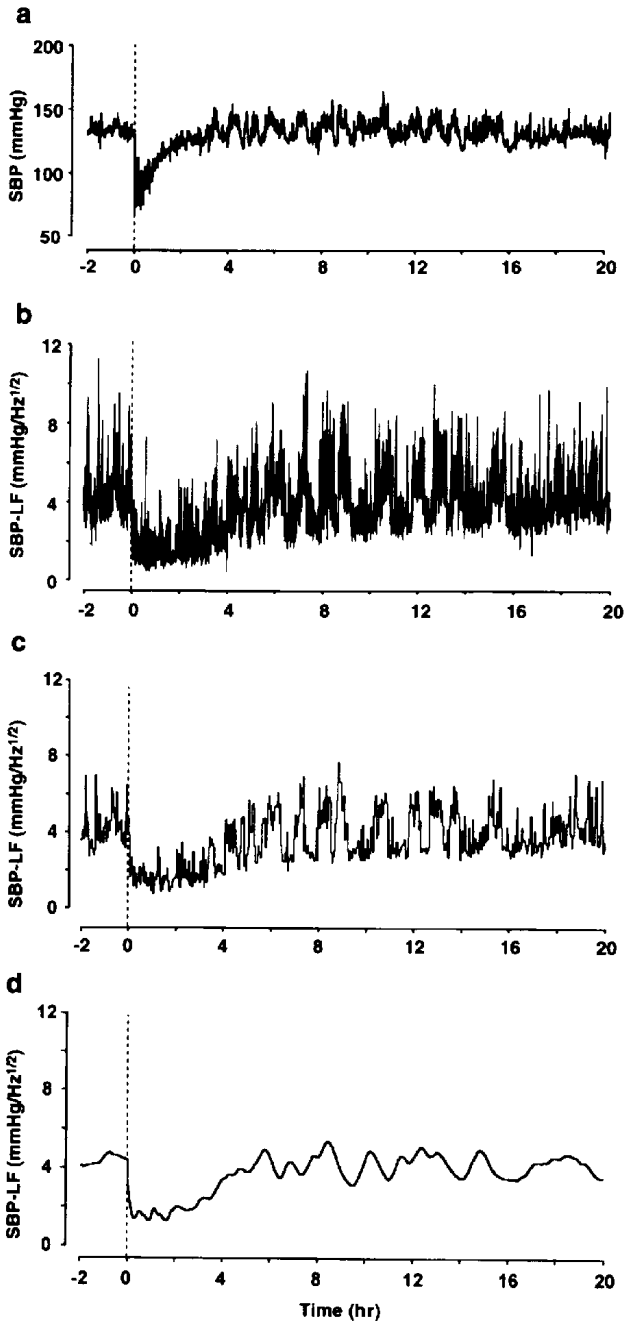

Fig. 5. Time course of SBP (a), SBP-LFamp in periodogram (b), SBP-LFamp calculated from the usual power spectral calculation method (c) and SBP-LFamp calculated from the weighted averaging method with digital filters (d). Phentolamine at 3 mg/kg, i.v. was administered at 0 hr as indicated by hashed lines.

manner: HR-HFamp was increased ($r=0.99$) at a low dose and decreased ($r=1.00$) at a high dose (Fig. 7a). Phentolamine decreased SBP-VLFamp ($r=0.99$) and SBP-LFamp ($r=0.98$) and increased SBP-HFamp ($r=0.99$) (Fig. 7b). Propranolol decreased HR and changed all amplitudes in the HR fluctuations in a dose-

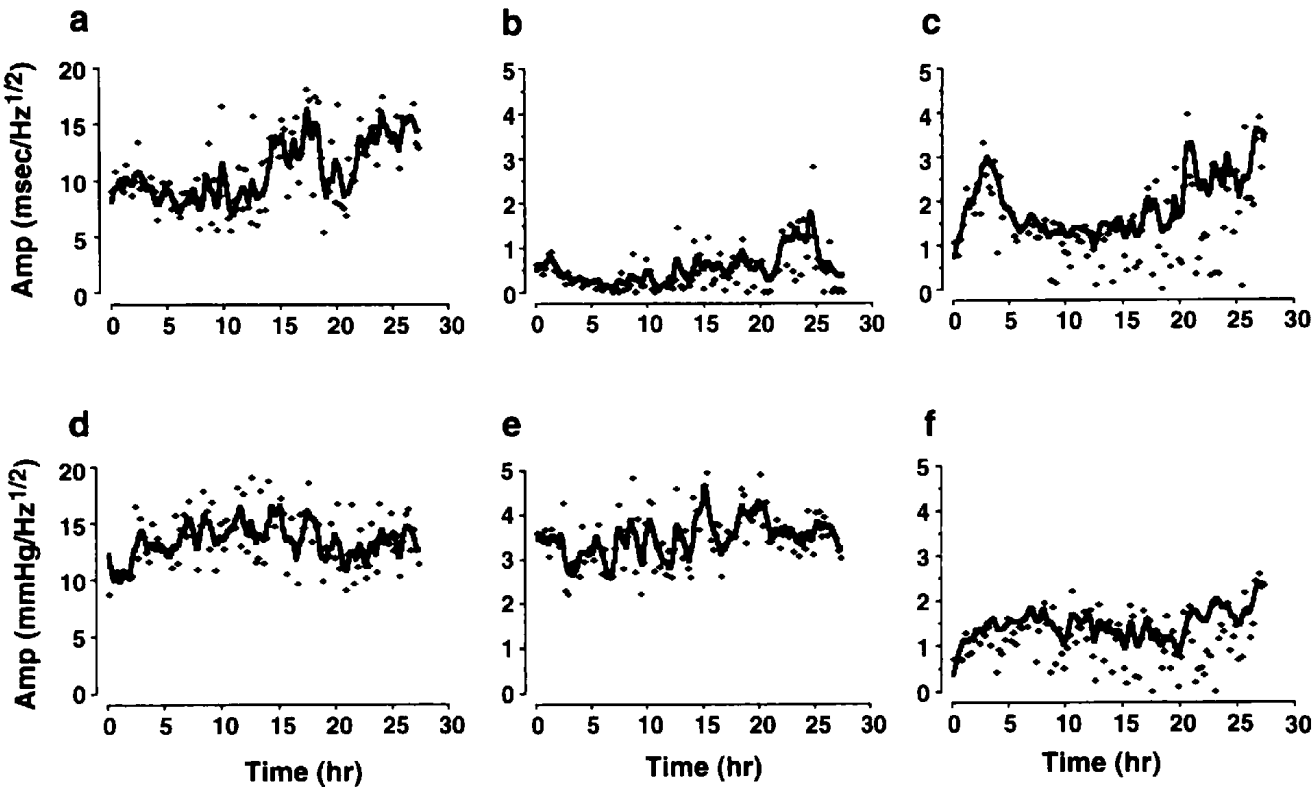

Fig. 6. Comparison between the weighted averaging method with digital filters and the existing calculation method. Solid lines show the time courses of the amplitudes calculated from the weighted averaging method with digital filters, and dots show the time courses of the amplitudes of the existing calculation method. a: HR-VLFamp, b: HR-LFamp, c: HR-HFamp, d: SBP-VLFamp, e: SBP-LFamp, f: SBP-HFamp.

dependent manner. HR change was used as an incidence for the calculation of r values. Propranolol decreased HR-LFamp ($r=0.96$) and SBP-LFamp ($r=0.98$) (Fig. 7: c and d). The decrease of HR-VLFamp and SBP-VLFamp by propranolol was not correlated quantitatively to the HR decrease (Fig. 7: c and d). Atropine increased HR and changed all amplitudes of the HR fluctuations in a dose-dependent manner. HR change was used as an incidence for the calculation of r values. Atropine decreased HR-VLFamp ($r=1.00$), HR-LFamp ($r=1.00$) and HR-HFamp ($r=1.00$); however, atropine did not change any amplitudes in MBP (Fig. 7e). These results are summarized in Table 1.

DISCUSSION

The findings in this study demonstrate the importance of real-time, continuous and accurate quantitative analysis. This system was designed to resolve two key problems in real-time analysis of plural indexes (HR, SBP, MBP and DBP) in conscious rats, high-speed processing and accurate noise-adjusted power spectrum calculation.

With the first problem, in general in order to achieve real-time FFT, only one index at a time can be processed, i.e., HR or BP, because of the slow processing rate of the FFT. For real-time FFT of plural parameters, high-speed processing is essential (18). In this study, continuous plural data transfer to the FFT calculation function was effectively controlled by object-oriented programming. Moreover, the system's high-speed processing capabilities allowed real-time recognition of WIs with BP waveform segmentation by digital filters to be achieved. Assembler and C++ was combined since C++ alone could not achieve sufficient processing speed.

With respect to the second problem, the system was able to realize accurate noise-adjusted power spectral calculations. In this study, digital filters and Smirnov's rejection test were used for BP waveform segmentation and outliers rejection (18), respectively. To calculate the power amplitude area, current methods can only calculate a single power spectrum every several minutes by calculating a simple average of each periodogram. Calculating an arithmetical average of several periodograms causes discontinuity in calculating power spectra for several minutes (1) and can not reject an abnormal periodogram (Fig. 4c). However, because the system calculates the

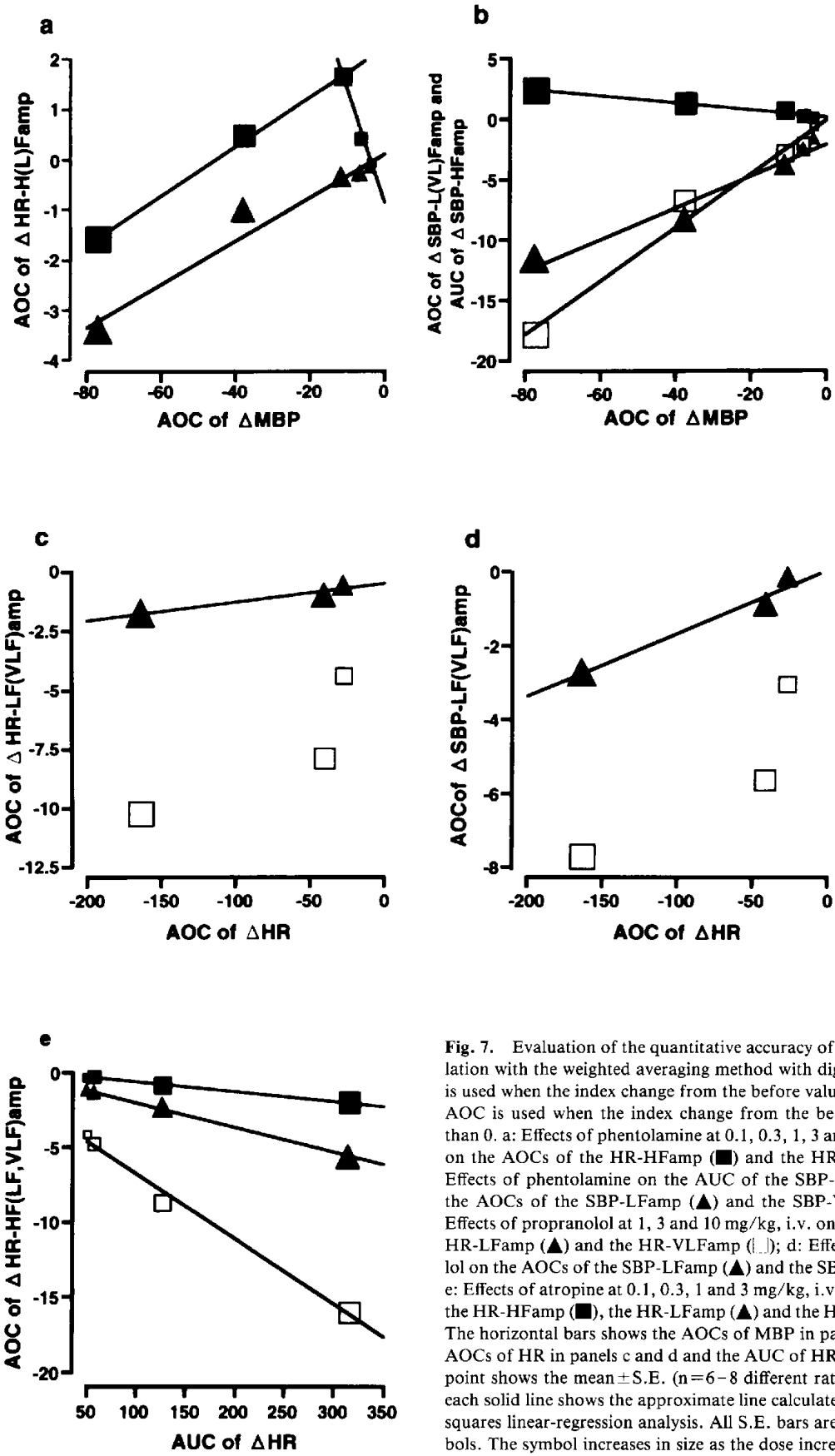

Fig. 7. Evaluation of the quantitative accuracy of amplitude calculation with the weighted averaging method with digital filters. AUC is used when the index change from the before value is more than 0. AOC is used when the index change from the before value is less than 0. a: Effects of phentolamine at 0.1, 0.3, 1, 3 and 10 mg/kg, i.v. on the AOCs of the HR-HFamp (■) and the HR-LFamp (▲); b: Effects of phentolamine on the AUC of the SBP-HFamp (■) and the AOCs of the SBP-LFamp (▲) and the SBP-VLFamp (□). c: Effects of propranolol at 1, 3 and 10 mg/kg, i.v. on the AOCs of the HR-LFamp (▲) and the HR-VLFamp (▯); d: Effects of propranolol on the AOCs of the SBP-LFamp (▲) and the SBP-VLFamp (□). e: Effects of atropine at 0.1, 0.3, 1 and 3 mg/kg, i.v. on the AOCs of the HR-HFamp (■), the HR-LFamp (▲) and the HR-VLFamp (□). The horizontal bars shows the AOCs of MBP in panels a and b, the AOCs of HR in panels c and d and the AUC of HR in panel e. Each point shows the mean ± S.E. (n = 6–8 different rats) at a dose, and each solid line shows the approximate line calculated from the least-squares linear-regression analysis. All S.E. bars are behind the symbols. The symbol increases in size as the dose increases.

Table 1. Amplitude change of each frequency component

a. Drug	Phentolamine	Propranolol	Atropine
HR	↑	↓	↑
MBP	↓	···	···
HR-VLF	↓	↓	↓
HR-LF	↓	↓	↓
HR-HF	↑(↓)	···	↓
SBP-VLF	↓	↓	···
SBP-LF	↓	↓	···
SBP-HF	↑	···	···

b. Drug	Phentolamine	Propranolol	Atropine
Index	MBP	HR	HR
HR-VLF	···	···	N
HR-LF	P	P	N
HR-HF	N (P)	···	N
SBP-VLF	P	···	···
SBP-LF	P	P	···
SBP-HF	N	···	···

a: ↑, ↓ and ··· shows increase, decrease and no change, respectively. ↑ (↓) shows increase at low dose and decrease at high dose.
b: P, N and ··· shows positive relation, negative relation and no change, respectively, to each index. N (P) shows a negative relation at low dose and a positive relation at high dose.

weighted average of a series of amplitude areas, using digital filters, the discontinuity interval was very short (25.6 sec after the half-overlap method is applied). We speculate that the interval of 25.6 sec is short enough so that it will not adversely affect proper drug evaluation. Moreover, it is possible for the weighted averaging method with digital filters to reject any abnormal periodogram in which data show a rectangular phase (Fig. 4d). For example, the rectangular phase corresponds to the artificial tachyarrhythmia for 2 sec. It was impossible to reject the continuous arrhythmia with the rejection test in the previous report (18). Accordingly, it was shown that the weighted averaging method with digital filters was effective for the data which had unrejected continuous arrhythmia. Furthermore, calculating the weighted average with digital filters guarantees continuity and accuracy for determining the actual representative values of the power amplitude (Figs. 4–6). Other characteristics of the system are its ability to reject the white noise component (baseline amplitude). In the simulation model, an elevation of the baseline amplitude by artificial white noise was rejected in this system (data not shown).

An interesting feature about this system is that it is able to detect the HFamp accurately, which most current methods have failed to do since they use the total HF area to calculate the HFamp. Furthermore, the frequency of the center part of the HF component changes greatly according to respiration rate. In conscious rats, the frequency of the center area is from 0.8 to 3 Hz, and the HFamp is much smaller than the LFamp and VLFamp. Accordingly, small changes in HFamp are undetectable by most current methods (Fig. 6). The system has a HF peak detection function that determines the HFamp at 0.26 Hz before and after the frequency center of the HF component. The method was effective during night-time measurement when rats are active and their respiration rate changes (Fig. 6).

Pharmacological tests were used for validating the accuracy of the system (Fig. 7). Phentolamine, propranolol and atropine were used because they are representative drugs for antagonizing α-adrenoceptors, β-adrenoceptors and muscarinic acetylcholine receptors, respectively. The changes of the power amplitudes of each frequency component vs the changes of the indexes which these drugs affect directly were plotted at each dose in Fig. 7. AUC or AOC of power amplitude and indexes were used for the plotted value because the evaluation with only one peak value has a possibility of generating more errors than that with AUC or AOC. The accuracy of the system was proved by the linearity ($r \geq 0.96$) of the plotting. In this study, SBP-LFamp was reduced by phentolamine and HR-HFamp was reduced by atropine in a dose-dependent manner. These results support that the system can measure total sympathetic function and total parasymapthetic function quantitatively.

Interestingly, unlike other systems, the HF peak detection and baseline rejection functions of the system allowed us to detect minute changes in HR-HFamp and SBP-HFamp after phentolamine administration, resulting in very accurate detection. In this study, phentolamine increased the SBP-HFamp and changed the HR-HFamp in a biphasic manner. It has been reported that venous return while in a tilted position affects the HFamp (3). We speculate that the dose-dependent increase in HR-HFamp and SBP-HFamp by phentolamine may have been caused by the phentolamine-induced reduction in venous return. The pharmacological and physiological meanings about the characteristic changes in the other components will need to be clarified further.

The high-speed processing and noise-adjusting power spectrum calculation capabilities of this system allowed for real-time and accurate determinations of BP and HR

fluctuations, which in turn increased the precision of drug evaluation in conscious rats. Furthermore, this accurate system enabled us to discover the biphasic change in HR-HFamp and the increase in SBP-HFamp in a dose-dependent manner caused by phentolamine, which has been difficult to detect until now.

Acknowledgments

The authors would like to thank Ms. F. Fukuya for her excellent experimental help; Ms. S. Thirion for her advice on the translation into English; and Drs. M. Shimizu, T. Karasawa, K. Hosoki, K. Takeyama and Y. Masuda for their encouraging support. We also thank Drs. T. Musha, Y. Ueda and E. Ohsuga for their valuable discussions and comments.

REFERENCES

1 Akselrod S, Gordon D, Ubel FA, Shannon DC, Barger AC and Cohen RJ: Power spectrum analysis of heart rate fluctuation: a quantitative probe of beat-to-beat cardiovascular control. Science **213**, 220–222 (1981)

2 Akselrod S, Gordon D, Madwed JB, Snidman NC, Shannon DC and Cohen RJ: Hemodynamic regulation: investigation by spectral analysis. Am J Physiol **249** (Heart Circ Physiol **18**), H867–H875 (1985)

3 Baselli G, Cerutti S, Civardi S, Liberati D, Lombardi F, Malliani A and Pagani M: Spectral and cross-spectral analysis of heart rate and arterial blood pressure variability signals. Comput Biomed Res **19**, 520–534 (1986)

4 De Boer RW, Karemaker JM and Strackee J: Relations between short term blood-pressure fluctuations and heart rate variability in resting subjects: I. a spectral analysis approach. Med Biol Eng Comput **23**, 352–358 (1985)

5 Hyndman BW, Kitney RI and Sayers BMcA: Spontaneous rhythms in physiologic control systems. Nature **233**, 339–341 (1971)

6 Kitney RI and Rompelman O: The Study of Heart-Rate Variability. pp 59–107, Oxford, Clarendon (1980)

7 Daniels FH, Leonard EF and Cortell S: Spectral analysis of arterial blood pressure in rat. IEEE Trans Biomed Eng BME-**30**, 154–159 (1983)

8 Sayers BMcA: Analysis of heart rate variability. Ergonomics **16**, 17–32 (1973)

9 Randall DC, Brown DR, Raisch RM and Randall WC: SA-nodal parasympathectomy delineates autonomic contributions to heart rate power spectrum. Am J Physiol **260** (Heart Circ Physiol **29**), H985–H988 (1991)

10 Randall DC, Randall WC, Yingling JD and Raisch RM: Heart rate control in awake dog after selective SA-nodal parasympathectomy. Am J Physiol **262** (Heart Circ Physiol **31**), H1128–H1135 (1992)

11 Brown DR, Brown LV, Patwardhan A and Randall DC: Sympathetic activity and blood pressure are tightly coupled at 0.4 Hz in conscious rats. Am J Physiol **267** (Reg Integrative Comp Physiol **36**), R1378–R1384 (1994)

12 Cerutti C, Gustin MP, Paultre CZ, Lo M, Julien C, Vincent M and Sassard J: Autonomic nervous system and cardiovascular variability in rats: a spectral analysis approach. Am J Physiol **261** (Heart Circ Physiol **30**), H1292–H1299 (1991)

13 Pagani M, Lombardi F, Guzzetti S, Rimoldi O, Furlan R, Pizzinelli P, Sandrone G, Malfatto G, Dell'Orto S, Piccaluga E, Turiel M, Baselli G, Cerutti S and Malliani A: Power spectrum analysis of heart rate and arterial pressure variabilities as a marker of sympatho-vagal interaction is man and conscious dog. Circ Res **59**, 178–193 (1986)

14 Kubota T, Itaya R, Alexander J Jr, Todaka K, Sugimachi M and Sunagawa K: Autoregressive analysis of aortic conscious rats: effects of autonomic blockers. J Auton Nerv Syst **30**, 91–100 (1990)

15 Person PB, Stauss H, Chung O, Wittmann U and Unger T: Spectrum analysis of sympathetic nerve activity and blood pressure in conscious rats. Am J Physiol **263** (Heart Circ Physiol **32**), H1348–H1355 (1992)

16 Rimoldi O, Pierini S, Ferrari A, Cerutti S, Pagani M and Malliani A: Analysis of short-term oscillations of R-R and arterial pressure in conscious dogs. Am J Physiol **258** (Heart Circ Physiol **27**), H967–H976 (1990)

17 Kuo Terry BJ and Chan Samuel HH: Continuous, on-line, real-time spectral analysis of systemic arterial pressure signals. Am J Physiol **264** (Heart Circ Physiol **33**), H2208–H2213 (1993)

18 Nagai R and Nagata S: New algorithmic-based digital filter processing system for continuous blood pressure measurement and analysis in conscious rats. Comput Biol Med **25**, 483–494 (1995)